Gas Transport Properties of Poly(Ethylene-2,6-Naphtalene Dicarboxylate) Films: Influence of Crystallinity and Orientation

L. Hardy, E. Espuche, G. Seytre, I. Stevenson

Laboratoire des Matériaux Polymères et des Biomatériaux, UMR CNRS no. 5627, Bâtiment ISTIL, Université Claude Bernard, LYON I, 43, Boulevarde du 11 Novembre 1918, 69622 Villeurbanne Cedex, France

Received 12 July 2002; accepted 17 September 2002

ABSTRACT: H_2 and CO_2 transport properties were investigated on semicrystalline poly(ethylene-2,6-dicarboxylate naphtalene) (PEN) films and biaxially stretched films and analyzed in terms of solubility and diffusion. The decrease of the permeability observed on the thermally crystallized samples has been described by Maxwell's law. No change of the sorption properties of the amorphous phase has been noticed as a function of the thermal treatment and the evolution of the diffusion coefficient has been related to a tortuosity effect. The low permeability measured on the biaxially stretched film is related to both a change of the free volume sizes distribution and a tortuosity effect. The interesting barrier properties of the biaxially stretched film are kept even after annealing the film at 250°C. © 2003 Wiley Periodicals, Inc. J Appl Polym Sci 89: 1849–1857, 2003

Key words: gas permeation; orientation; crystallization; diffusion

INTRODUCTION

In recent years, polymers have been extensively used in food packaging and beverage bottling industries that require low gas-permeable materials. The polymer is often under semicrystalline or oriented form to increase its barrier properties. In all cases, the gas sorption and diffusion processes, the two mechanisms at the origin of the gas transport, take place almost exclusively through the amorphous region but depend on the morphology.

It has been shown[1–4] that for semicrystalline polymers, the presence of isotropic crystalline phases does not affect the specific amorphous sorption but reduces the gas diffusion by a tortuosity effect and in some cases by an additional parameter: the reduction of the amorphous chain mobility.

Concerning the oriented samples,[5–12] a drastic reduction of gas permeability coefficients is often observed but sometimes conflicting explanations are given to describe this evolution, depending on the types of polymers studied.

According to Carfagna et al.,[6] the decrease of permeability noticed for oriented polystyrene is due to a decrease of both solubility and diffusion coefficients and thus to a decrease of free volume. For Wang and Porter,[7] a constant solubility is measured and the evolution of permeability is strongly related to the evolution of the gas diffusion, concluding that the total free volume remains unchanged but that the hole's size distribution is modified by the orientation process.

For semicrystalline polymers such as polyethylene,[4,8–10] the drawing process leads to a small increase in crystallinity, to a change in crystallite size and orientation that can affect the tortuosity and in consequence the diffusion, and to a change in chain mobility in the amorphous phase that can also affect the diffusion. The importance of each of these different effects on the gas transport properties depends on the draw ratio and also on the molecular size of the diffusing molecule. The same observations have been reported by El Hibri and Paul[11] on poly(vinylidene fluoride).

All these studies show the interest of studying the evolution of the transport properties, considering both the sorption and the diffusion mechanisms, and as a result, the permeation properties. It is also essential to relate these properties to the morphological changes that occur in the material after drawing.

In this study, the gas transport properties of polyethylene-2,6-dicarboxylate naphthalene (PEN) is evaluated. This polymer differs from poly(ethylene terephthalate) (PET) by the presence of the naphthalene group instead of the phenyl ring. Compared to PET, the presence of the naphthalene group in PEN gives rise to a higher glass transition temperature (T_g) and melting temperature values. PEN can also be considered as a potential candidate for the bottling of carbonated drinks, a packaging application where PET is already well established. If a lot of work has been developed for studying the gas transport prop-

Correspondence to: E. Espuche.

Journal of Applied Polymer Science, Vol. 89, 1849–1857 (2003)

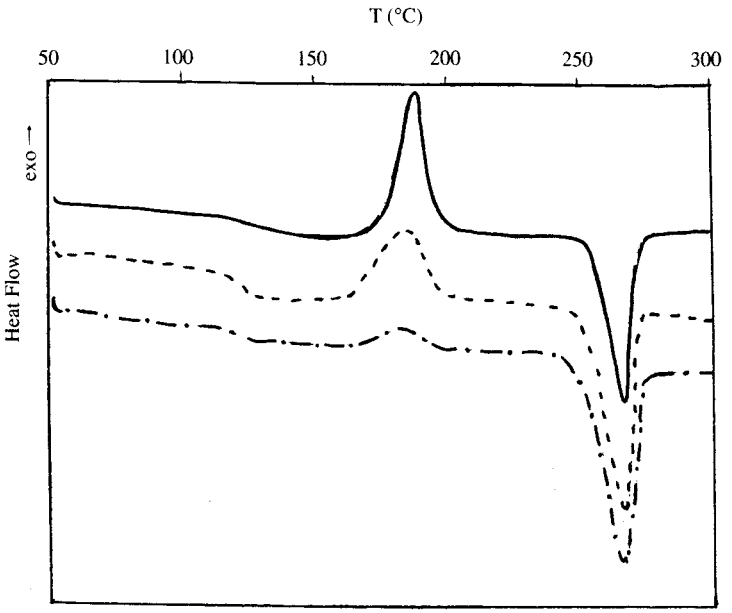

Figure 1 Evolution of the reference DSC thermogram as a function of treatment time at 154°C: (—) reference film, (- -) film treated for 20 min; (— - —) film treated for 40 min.

erties of PET,[12,13] only some articles have been concerned with the water transport in PEN,[14]and very few studies have dealt with its gas transport properties.[15] The aim of this work is thus to determine these gas transport properties, allowing a better understanding of the role of crystallinity and of orientation.

EXPERIMENTAL

Materials

Two types of PEN films, supplied by DuPont Ltd. (Luxembourg), were considered in this study.

The first type of film, a film with a thickness equal to 40 μm, obtained by cast film extrusion was taken as reference. This cast film was treated at 154°C, a temperature corresponding to the beginning of the cold crystallization. Because quite fully amorphous isotropic samples were used to obtain the crystalline ones, orientation effects on the properties could be excluded for these samples. Varying the times at 154°C led to various crystallinity degrees.

The second type of film we considered was a biaxially stretched sample with a thickness equal to 25 μm. It was obtained by using an extrusion machine which allows the PEN film to be stretched sequentially in two directions (at 90° to each other), machine direction (MD) and transverse direction (TD), respectively. A previous work,[16] consisting of the study of the pole figures from WAXS experiments, has shown that in this film the crystalline entities were at 45° to MD and TD and also parallel to the plane of the film and perpendicular to MD. Two annealing treatments were applied to this film. The first one consisted of heating the sample from room temperature to 240°C at a heating rate of 20°C/min. The annealing time was 1 h and after that period, the sample was slowly cooled to room temperature at a rate of −5°C/min. The second treatment differed from the first one by the value of the plateau temperature: 250°C.

DSC measurements

DSC experiments were performed on samples of about 10 mg by using a Perkin–Elmer apparatus with a heating rate of 10°C/min from 50 to 300°C. Figure 1 shows the thermograms obtained for the reference film and the isotropic semicrystalline films. Two parameters were determined from the thermograms, the T_g at the onset on base line change of the heat capacity and the crystallinity degree. To determine this last parameter, the crystallization exothermic enthalpy, $\Delta H_{\text{cold crystallization}}$ or ΔH_c, was subtracted from that of the melting endotherm, $\Delta H_{\text{melting}}$ or ΔH_m. Crystallinity of the films (X_c) was calculated according to:

$$X_c = 100 \times (\Delta H_m - \Delta H_c)/\Delta H_\infty \qquad (1)$$

Two values of ΔH_∞ can be found in the literature for PEN, 103.4 J/g[17] and 190 J/g,[18] respectively. Some authors[19,20] have compared results obtained by density measurements and DSC measurements and have deduced that the value of 103.4 J/g was too low to obtain good results. We have then chosen to take ΔH_∞ as equal to 190 J/g.

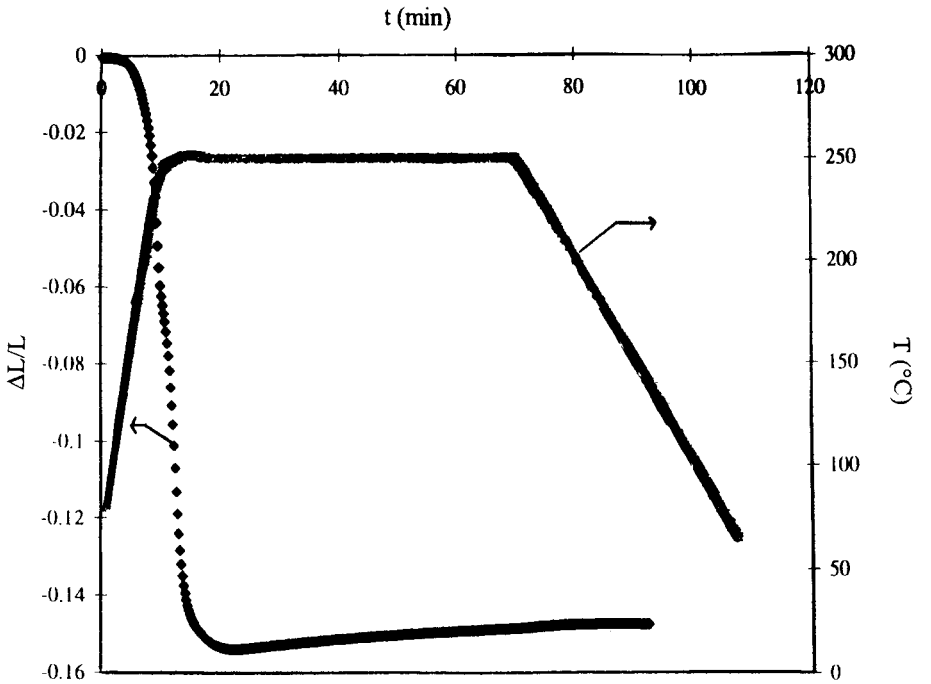

Figure 2 Evolution of the shrinkage measured on the biaxially stretched film for the following thermal treatment: heating the sample from room temperature to 250°C at a heating rate of 20°C/min, maintaining the sample at 250°C for 1 h, and cooling the sample to room temperature at 5°C/min.

TMA measurements

TMA experiments were carried out on the biaxially drawn film by using a TA Instrument apparatus (DMA 2980 used in TMA mode). The same temperature ramps as for thermal treatments were used: heating the sample at 20°C/min from room temperature to a plateau temperature (240 or 250°C).The sample was maintained at the plateau temperature for 1 h and then slowly cooled to room temperature. Shrinking of the samples in the MD was recorded simultaneously as a $10^{-2}N$ force was applied to the sample. Figure 2 shows the evolution of the shrinkage measured on the biaxially stretched sample for a plateau temperature equal to 250°C.

Transport properties

Gas permeation analysis

The permeation cell consists of two compartments separated by the studied membrane (useful area: 3 cm^2). The cell was thermostated at 20°C. A preliminary high-vacuum desorption was performed to ensure that the static vacuum pressure changes in the downstream compartment were smaller than the pressure changes due to the gas diffusion.

A 3×10^5 Pa gas pressure was then introduced in the upstream compartment. The pressure variations in the downstream compartment are measured with a datametrics pressure sensor. A steady-state line was obtained after a transitory state by plotting the measured pressure versus time. The permeability coefficient expressed in barrer units (1 barrer = 10^{-10} cc_{STP} $cmcm^{-2}$ s^{-1} $cm_{Hg}{}^{-1}$) was calculated from the slope of the steady-state line. The precision of the values was better than 10%.

The diffusion coefficient D (cm^2 s^{-1}) was deduced from the time lag, θ, provided by the extrapolation of the steady-state line on the time axis:

$$D = \frac{e^2}{6\theta} \tag{2}$$

where e is the thickness of the film.

The transport of the two gases differing by their molecular size and their interaction capacity toward glassy polymers was evaluated: hydrogen is a small and low interactive gas, whereas carbon dioxide is a bigger and a higher interactive gas.

Gas sorption analysis

The specimens were introduced in a SETARAM B92 microbalance. After desorption under vacuum (3×10^{-6} mbar) at a constant temperature (20°C), a gas pressure in the range 0–760 torrs was established within the apparatus and the gas uptake was followed as a function of time until equilibrium was attained. The balance precision was equal to 1 μg.

The sorption isotherm was determined from the weight uptake at the sorption equilibrium. Furthermore, the evolution of the weight uptake as a function of time gave information on the kinetics of the sorption. The diffusion coefficient D was deduced from Fick's second law:

$$-\frac{\partial c}{\partial t} = D\frac{\partial^2 c}{\partial x^2} \tag{3}$$

where c is the gas concentration of the sorbed molecules, t is the time, and x is the position in the film.

By introducing the following boundary conditions, concentration of sorbed molecules equal to 0 for $t = 0$ at each point of the specimen except at the surface where the equilibrium is reached instantaneously, a simplified solution of the Fick's equation was obtained:

$$\frac{M_t}{M_\infty} = 1 - \frac{8}{\Pi^2}\sum_{n=0}^{\infty}\frac{1}{(2n+1)^2}\exp\frac{-\Pi^2(2n+1)^2 Dt}{e^2} \tag{4}$$

where M_t is the gas sorbed at the time t and M_∞ is the gas sorbed at the sorption equilibrium.

The value of D was computed by iterative calculations leading to the best fit of experimental data by the theoretical eq. (4).

RESULTS

Isotropic crystallized PEN films

Before studying the effect of the different treatments applied to PEN, the crystallinity, the permeability, and the sorption properties of the reference film were determined. The results are presented in Table I. The reference film is not totally amorphous but its crystallinity remains low (2%).

As expected, the permeation data emphasize the good barrier properties of PEN. Indeed, the H_2 and CO_2 permeability coefficients are, respectively, in the range of 0.9 and 0.12 Barrer, and the CO_2 diffusion coefficient determined by the time lag method is equal to 1.35×10^{-10} cm^2 s^{-1}.

TABLE I
Properties of Isotropic Semicrystalline PEN

	Treatment time at 154°C (min)			
	0	20	40	50
X_c (%)	2	9	19	22
Pe H_2 (barrer)	0.9	0.77	0.55	0.45
PeCO_2 (barrer)	0.127	0.104	0.077	0.06
D CO_2 (10^{-11} cm^2/s)	13.5	10	8.7	7.5

X_c, crystallinity; Pe, permeability coefficient; D, diffusion coefficient.

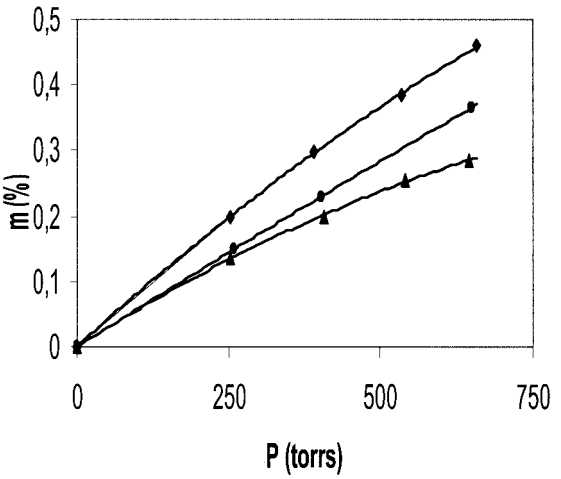

Figure 3 CO_2 sorption isotherm (♦) of the 40 μm reference film, (●) of the isotropic semi crystalline film with X_c = 19%, and (▲) of the biaxially drawn sample.

Sorption experiments were carried out on this reference film with the most interactive gas, CO_2.

From the CO_2 uptakes determined at the equilibrium at different pressures, the CO_2 sorption isotherm represented in Figure 3 was obtained. It is curved toward the pressure axis and is thus representative of a dual-mode sorption, indicating an addition of two contributions: the Langmuir's type sorption with high interactions on specific sites or in unrelaxed volumes and the Henry's type mixing. The concentrations of CO_2 molecules sorbed according to each of these mechanisms are noted as C_H and C_D, respectively, and they can be expressed as a function of the pressure,

$$C_H = C'_H bP/(1 + bP) \tag{5}$$

$$C_D = k_D P \tag{6}$$

where P is the equilibrium gas pressure, k_D is the Henry's law solubility constant, b is the Langmuir affinity constant, and C_H' is the Langmuir capacity constant.

Thus, the total gas concentration C sorbed by the glassy polymer is

$$C = C_D + C_H = k_D P + \frac{C_H' bP}{1 + bP} \tag{7}$$

Sorption data were fitted by eq. (7) to determine the parameters of the model. The following values were obtained: K_D = 2.16 cm_{STP}^3 cm^{-3} atm^{-1}, C_H' = 2.6 cm_{STP}^3 cm^{-3}, and b = 0.94 atm^{-1}. These values result from the fitting of the sorption isotherm in a quite narrow range of CO_2 pressures and are nevertheless in

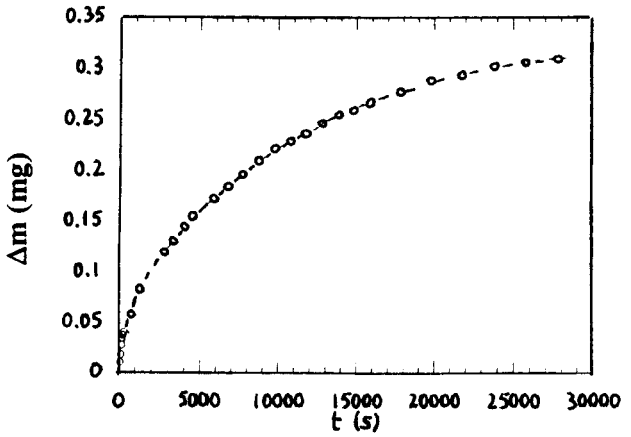

Figure 4 Comparison between (○) experimental and (- -) theoretical CO_2 uptakes at a pressure equal to 650 Torr for a 70-mg sample of the 40 μm reference film.

good agreement with the values reported by Brolly et al.[15]

To determine kinetic parameters from sorption data, the evolutions of CO_2 uptakes as a function of time were fitted at different CO_2 pressures by the theoretical eq. (4). As shown in Figure 4, the agreement between experimental and theoretical points is very good. A Fickian mechanism thus governs the PEN transport properties and allows the determination of the diffusion coefficients. The values obtained for CO_2 pressures ranging from 0 to 760 torrs are presented in Table II. In the dual mode, the diffusion coefficient generally increases as the pressure increases and as the Henry's mode is mainly acting. This trend is verified for the reference PEN film but the variations of D are not very important. The obtained D values confirm the results obtained by permeation (e.g., the low diffusive character of the reference PEN).

Table I presents the treatments applied to the 40-μm-thick reference membrane. The crystallinity degree, the permeability, and the diffusion coefficients determined for H_2 and CO_2 after the different treatments are also reported. According to the literature, PEN can crystallize under two triclinic forms, α and β.[21,22] The α-form corresponds to one chain per unit cell and is easily obtained from crystallization at 160°C after melting at 280°C. The β-form has two chains per unit cell in which the naphthalene group undergoes a 180° rotation around the bond axis linking the carbon atoms in the 4 and 4′ positions. The β-form can only be obtained in more specific conditions than α-form (e.g., by melting the sample above 330°C followed by a

TABLE II
CO_2 Sorption Properties of the Reference film

P (torrs)	250	390	530	660
CO_2 uptake (%)	0.2	0.3	0.38	0.46
D (10^{-11} cm^2/s)	12.2	12.7	13	13.2

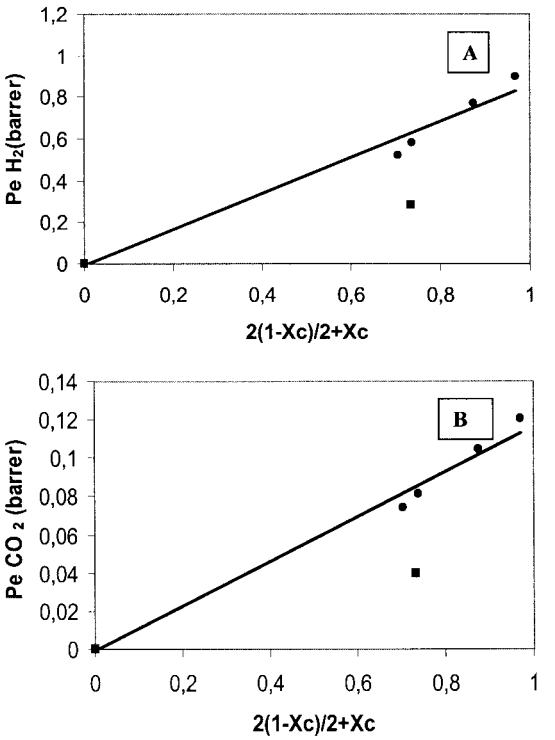

Figure 5 Evolution of the permeability coefficient for (A) H_2 and (B) CO_2 as a function of $2(1 - X_c)/(2 + X_c)$. (●) is representative of isotropic semicrystalline samples, (■) is representative of the biaxially drawn sample.

crystallization at 245°C reached after a rapid cooling). In our crystallization conditions, α-form was nucleated and an increase of the treatment time led to an increase of the crystallinity X_c and to a small variation of the T_g (Table I and Fig. 1).

As a general trend, the permeability decreases as the crystallinity increases. In the case of isotropic semicrystalline material, the crystalline zone has been often represented by dispersed impermeable spheres in a permeable matrix. According to this representation, the simplified Maxwell law[23] should be used and the dependence of P_e should be proportional to $2(1 - X_c)/(2 + X_c)$. Good agreement is noticed between experimental and theoretical values. The extrapolation of the experimental straight line to $X_c = 0$ allows the determination of the permeability coefficients for a totally amorphous PEN film: 0.9 and 0.12 Barrer for H_2 and CO_2, respectively (Fig. 5).

To determine the role of the solubility and diffusion in the decrease of the permeability as a function of the crystallinity, the CO_2 sorption properties were evaluated for the sample treated for 40 min at 154°C. This treatment leads to a crystallinity degree equal to 19%. The CO_2 diffusion coefficients determined in the range of pressures between 0 and 700 torrs increased from 7 to 8×10^{-11} cm^2 s^{-1} when the pressure increased. The diffusion is thus slower than for the reference film. The CO_2 uptakes are also lower than in the case of the

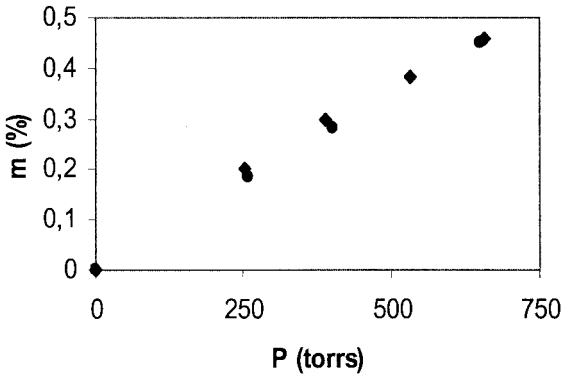

Figure 6 Comparison between the CO_2 uptakes of (♦) the 40 μm reference film and the CO_2 uptakes expressed as a function of the lonely amorphous phase for (●), the isotropic semicrystalline PEN with X_c = 19%.

reference film (Fig. 3). Nevertheless, these uptakes expressed as a function of the lonely permeable phase (e.g., the amorphous phase) determine an isotherm identical to the reference one (Fig. 6). Thus, for isotropic semicrystalline PEN films, one can verify that

$$S = S_a(1 - X_c) \tag{8}$$

where S_a is the solubility of the amorphous phase and X_c the crystallinity of the sample.

The decrease of solubility observed for the semicrystalline samples is thus directly related to the decrease of the permeable amorphous fraction. The sorption capacity of this phase is not modified by the thermal treatments that have been applied to the films. In conclusion, the distribution of holes' sizes devoted to the sorption mechanism is the same for all samples even after a thermal treatment leading to isotropic semicrystalline films.

The sorption experiments have emphasized a decrease of the diffusion rate between the reference film and the 19% semicrystalline film. This trend is confirmed by the permeation data: a decrease of the CO_2 diffusion coefficient is observed as the crystallinity increases (Table I). This transport parameter is dependent on both the size of the diffusing molecule and the structure and morphology of the polymer. According to the literature,[24] D is related to D_a, the diffusion coefficient relative to the amorphous phase by the equation:

$$D = D_a/\tau\beta \tag{9}$$

where τ is representative of the tortuosity of the path due to the presence of impermeable crystalline components and has the same effect on all gases and β is related to the mobility of the chains in the amorphous phase. In the case of isotropic semicrystalline materials, a lack of mobility in the amorphous regions close to the anchoring points in the crystals can be noticed. A consequent increase in chain immobilization can have the effect of reducing the diffusion coefficient for the larger gas molecule while not affecting the smallest ones. This last effect was noticed by Webb et al.[9] on drawn polyethylene.

In this study, $\tau\beta$ was evaluated for H_2 and CO_2 by using the permeability coefficients. In fact, the thicknesses of the films were too small to determine a diffusion coefficient with a good precision for H_2. However, it has been verified that for all the samples studied, a Fickian mechanism governs the gas transport, allowing the use of the equation:

$$P_e = DS \tag{10}$$

Furthermore, it has been shown that for semicrystalline samples,

$$S = S_a(1 - X_c),$$

As a consequence, $P_{ea}(1 - X_c)/Pe$ should be equal to $\tau\beta$.

In this study, P_{ea} was taken as the permeability extrapolated to $X_c = 0$ using the permeability coefficients of the isotropic crystallized samples. As a consequence, the evolution of $P_{ea}(1 - X_c)/P_e$ represented in Figure 7 will be only discussed on a qualitative basis. As a general trend, it can be remarked that $\tau\beta$ increases with X_c. Nevertheless, no significant influence on the nature of the diffusing molecule can be observed. This result is expected because both H_2 and CO_2 permeability coefficients follow Maxwell law, and in that case, $\tau\beta$ becomes equal to $1 + X_c/2$. The decrease of diffusion and permeability therefore appears to be more related to a tortuosity factor than to an immobilization effect. In contrast to polyethylene, the glass transition of amorphous PEN is high (equal to about 124°C) and permeability measurements are still made at room temperature in glassy state well

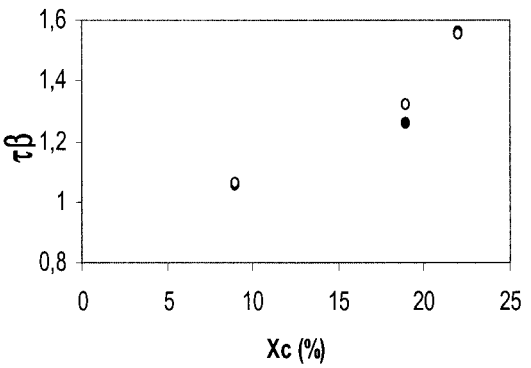

Figure 7 Evolution of $\tau\beta$ for H_2 and CO_2 for isotropic semicrystalline samples. The filled symbols are representative of CO_2 results.

TABLE III
Properties of Biaxially Drawn Samples

	Thermal treatment		
		1 h at 240°C	1 h at 250°C
Pe H_2 (barrer)	0.28	0.25	0.24
Pe CO_2 (barrer)	0.04	Not measured	0.03
D CO_2 (10^{-11} cm^2/s)	4	Not measured	3
X_c (%)	20	26	28

X_c, crystallinity; Pe, permeability coefficient; D, diffusion coefficient.

below T_g. Furthermore, the thermal treatments led to a small increase of T_g with the treatment time at 154°C (Fig. 1) and does not significantly affect the transport properties of small gases at room temperature.

Biaxially oriented PEN films

Table III presents the characteristics of the different samples. The 25-μm-thick biaxially oriented film has a crystallinity equal to 20%. Its T_g cannot be clearly identified because of a very low change of heat capacity (Fig. 8). The gas transport properties determined on this sample were compared to those measured on the isotropic semicrystalline sample studied in the preceding part and having the same crystallinity degree. The H_2 and CO_2 permeability coefficients measured on the biaxially stretched film are almost equal to half the values determined for the isotropic semicrystalline sample (Table III) and a quite similar decrease is observed on the diffusion coefficient (Tables I and III). For the biaxially stretched sample, the particular orientation of the crystalline entities proven in a previous morphological study[16] (e.g., at 45° to the machine and transverse direction and parallel to the plane of the film and perpendicular to the machine direction) induces a more tortuous gas path than in the case of the isotropic semicrystalline material. As a consequence, the permeability relative to the biaxially stretched film lowers the theoretical Maxwell law, considering a dispersion of impermeable spheres in the amorphous continuous matrix (Fig. 5). It also lowers the theoretical law representative of the gas diffusion through the amorphous phase containing dispersed and long impermeable cylinders perpendicular to the flux (Fig. 9). A lonely tortuosity effect cannot be at the origin of this result and an additional factor, the solubility, has to be taken into account. The effect of the bi-orientation process is less important on the CO_2 sorption isotherm (Fig. 3) than on the diffusion coefficient; nevertheless for the same crystallinity ($X_c \approx 20\%$), the CO_2 uptakes decrease by about 20% going from the isotropic semicrystalline sample to the bi-oriented one. The orientation process thus induces a change of the repartition of the free elementary vol-

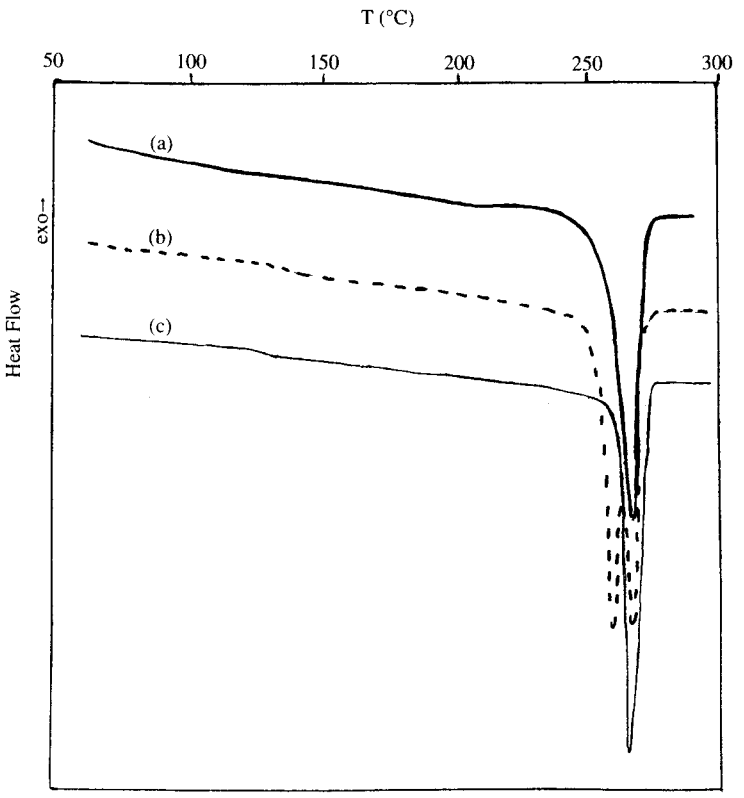

Figure 8 Effect of the annealing treatment at 240 and 250°C on the DSC biaxially oriented PEN thermogram: (a) biaxially oriented film; (b) 240°C annealed film; (c) 250°C annealed film.

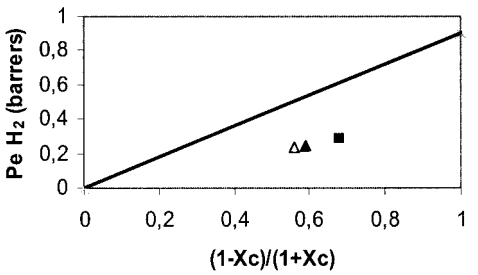

Figure 9 Evolution of the permeability coefficient for H_2 as a function of $(1 - X_c)/(1 + X_c)$, (■) is representative of the biaxially drawn sample, (▲) is representative of the film annealed at 240°C, and (△) is representative of the film annealed at 250°C.

umes leading to a modification of the sorption capacity of the amorphous phase. This effect associated with the high tortuosity induced by the orientation of the crystalline entities in the biaxially stretched sample can explain the low permeability observed. Tant et al.[25] have also revealed a change of the free volumes size and concentration in uniaxially oriented PEN and have attributed the particularly low permeability of these samples compared to PET to a morphological structure more typical of a liquid crystal polymer. Our results are thus in agreement with those of Tant et al., but compared to the uniaxially orientation process, our biaxially orientation process certainly leads to a more complicated morphology.

To know if these low values of flux can be kept after annealing of the films, the effects of two thermal treatments differing by their plateau temperature have been evaluated on the transport properties of the biaxially drawn film. These annealing temperatures, 240 and 250°C, respectively, are located at the beginning of the melting peak. During these treatments, the evolution of the shrinkage in the machine direction is registered and an example of the curves obtained is presented in Figure 2. A significant evolution of the shrinkage is noticed during the heating of the sample and during the first few minutes at the plateau temperature. Thereafter, it stabilizes at a value equal to ~ 9.5% for the treatment at 240°C and 15% for the treatment at 250°C. After these treatments, it is possible to detect much more easily the T_g of the samples. It is in the range of 120°C, whatever the treatment temperature (Fig. 8). Thus, both TMA and DSC results indicate that the annealing of the biaxially oriented film allows a relaxation of the amorphous phase and a gain in the chain mobility. Nevertheless, these effects do not vary to a great extent with the increase of the annealing temperature in the range of 240–250°C.

After the treatments, an increase of the crystallinity can be observed. The crystallinity degree becomes equal to about 27% after annealing, whatever the treatment temperatures between 240 and 250°C. Nevertheless, we notice that two different populations of crystallites appear under annealing at 240°C, leading to two distinct melting peaks located at 255 and 270°C, respectively (Fig. 8). The peak at 255°C is not observed for samples annealed at 250°C. For some authors,[26] this peak is expected to reflect the temperature of annealing of PEN film in the industrial process (also called thermosetting temperature and chosen 10 to 30°C below melting temperature, used to make the film more stable for heat shrinkage). According to Schoukens and Verschuere,[27] who worked on PEN samples uniaxially drawn at 145°C, the melting temperature of this low peak varies linearly with the shrinkage temperature from 228.4°C for a shrinkage temperature of 220°C to 249.5°C for a shrinkage temperature of 240°C.

The thermal treatments applied to the biaxially drawn sample led to a very small variation of the permeability coefficient. In fact, the annealing treatments have two effects with opposite consequences on the permeability: the increase of the chain mobility should lead to an increase of the permeability level and the increase of the impermeable crystalline fraction should lead to a decrease of the gas flux. The result is a very slight decrease on the permeability value showing the major role of the crystallinity. Furthermore, no effect of the small crystallites produced with a low degree of perfection and a corresponding low melting temperature during annealing and shrinkage of the film at 240°C is observed. The lonely global crystallinity degree seems to have an influence on the permeability. In conclusion, the very low permeability value of PEN is kept even after thermal treatments at high temperatures.

CONCLUSION

The H_2 and CO_2 transport properties of isotropic semicrystalline PEN films and biaxially oriented PEN films were evaluated and analyzed in terms of permeability, solubility, and diffusion. In both cases, a decrease of the permeability coefficient is noticed compared to the reference cast film, which is quasi-amorphous. This decrease is higher in the case of the biaxially drawn samples.

The evolution of the permeability is related to a decrease of both the solubility and the diffusion coefficients. Nevertheless, for the semicrystalline samples, the specific amorphous sorption is equivalent to that of the reference film and the decrease of the diffusion coefficient is more closely related to a tortuosity effect than to an effect of a lack of mobility in the amorphous phase. For the biaxially stretched films, the tortuosity effect is more important because of the particular orientation of the crystalline entities and a decrease of the sorption capacity has been evidenced in the amorphous phase. The association of these two effects explain the low permeability values measured on the

biaxially oriented film. Annealing this film at temperatures ranging from 240 to 250°C led to an increase of chain mobility and an increase of the crystallinity. These parameters have opposite effects on the permeability and finally no great variation of the gas flux are observed after these treatments, showing that annealing at higher temperature are needed to drastically modify the transport parameters of the biaxially drawn PEN.

References

1. Michaels, A. S.; Vieth, W. R.; Bixler, H. J. J Appl Polym Sci 1964, 3, 2735.
2. Michaels, A. S.; Parker, R. E. J Polym Sci 1959, 41, 53.
3. Michaels, A. S.; Bixler, H. J. J Appl Polym Sci 1961, 50, 413.
4. Yasuda, H.; Peterlin, A. J Appl Polym Sci 1974, 18, 531.
5. Orchard, G. A. J.; Ward, I. M. Polymer 1992, 33, 4207.
6. Carfagna, C.; Nicodemo, L.; Nicolais, L.; Campanile, G. J Polym Sci, Polym Phys Ed 1986, 24, 1805.
7. Wang, L. H.; Porter, R. S. J Polym Sci, Polym Phys Ed 1984, 22, 1645.
8. Holden, P. S.; Orchard, G. A. J.; Ward, I. M. J Polym Sci, Polym Phys Ed 1985, 23, 709.
9. Webb, J. A.; Bower, D. I.; Ward, I. M.; Cardew, P. T. J Polym Sci, Polym Phys Ed 1993, 31, 743.
10. Sha, H.; Harrisson, I. R. J Polym Sci, Polym Phys Ed 1992, 30, 915.
11. El-Hibri, M. J.; Paul, D. R. J Appl Polym Sci 1986, 31, 2533.
12. Qureshi, N.; Stepanov, E. V.; Schiraldi, D.; Hiltner, A.; Baer, E. J Polym Sci, Polym Phys Ed 2000, 38, 1679.
13. Sekelik, D. J.; Stepanov, E. V.; Nazarenko, S.; Schiraldi, D.; Hiltner, A.; Baer, E. J Polym Sci, Polym Phys Ed 1999, 37, 847.
14. Rueda, D. R.; Varkalis, A. J Polym Sci, Polym Phys Ed 1995, 33, 2263.
15. Brolly, J. B.; Bower, D. I.; Ward, I. M. J Polym Sci, Polym Phys Ed 1996, 34, 769.
16. Douillard, A.; Hardy, L.; Boiteux, G.; Stevenson, I.; Seytre, G.; Galeski, A.; Kazmierczac, T. IUPAC MACRO 2000; Varsovie, Poland, 9–14 July 2000.
17. Cakmak, M.; Lee, S. W. Polymer 1995, 36 (21), 4039.
18. Buchner, S.; Wiswe, D.; Zachmann, H. G. Polymer 1989, 30, 480.
19. Cakmak, M.; White, J. L.; Spruiell, J. E. J Polym Eng Sci 1986, 6, 291.
20. Cakmak, M.; Kim, J. C. J Appl Polym Sci 1997, 64, 729.
21. Mencik, Z. Chemicky Prûmysil 1967, 17 (42), 2.
22. Buchner, S.; Wiswe, D.; Zachmann, H. G. Polymer 1996, 37, 3945.
23. Barrer, R. M. Diffusion in Polymers; Crank, J., Park, G. S., Eds., Academic Press: London/NewYork, 1968; Chapter6.
24. Holsti-Miettinen, R. M.; Pertila, K. P.; Seppala, J. V.; Heino, M. T. J Appl Polym Sci 1995, 58, 1551.
25. Tant, M. R.; Stewart, M. E.; Weinhold, S.; Long, J. V.; Hill, A. J. Polym Mater Sci Eng 1999, 81, 374.
26. Hardy, L.; Fritz, A.; Stevenson, I.; Boiteux, G.; Seytre, G.; Schônhals, A. J Non-Cryst Solids 2002, 305 (1–3), 174.
27. Schoukens, G.; Verschuere, M. Polymer 1999, 40; 3753.